Published in Current Applied Physics, DOI: 10.1016/j.cap.2024.11.012, online on 22 November 2024, Vol. 70, pp. 76-80.

Nanosecond electric pulse-induced ultrafast piezoelectric responses in Co^{3+} substituted $BiFeO_3$ epitaxial thin films

Sanjith Unithrattil[a,§], Taewon Min[b,§], Gopinathan Anoop[a,c], Jun Young Lee[a], Tae Yeon kim[a,d], Shibnath Samanta[a], Yubo Qi[e], Jiahao Zhang[e], Seung Hyun Hwang[a], Hyeon Jun Lee[f], Kun Guo[g], Su Yong Lee[h], Yasuhiko Imai[i], Osami Sakata[j], Keisuke Shimizu[k], Kei Shigematsu[k,l], Hajime Hojo[m], Kui Yao[g], Masaki Azuma[k,l], Jaekwang Lee[b], Andrew M. Rappe[e], and Ji Young Jo[a]

[a]School of Materials Science and Engineering, Gwangju Institute of Science and Technology, Gwangju- 61005, South Korea.

[b]Department of Physics, Pusan National University, Busan 46241, South Korea.

[c]Department of Physics, Amrita Vishwa Vidyapeetham, Amritapuri 690525, Kerala, India.

[d]Department of Materials Science and Engineering, University of California, Berkeley, Califronia- 94720, USA

[e]Department of Chemistry, University of Pennsylvania, Philadelphia, Pennsylvania 19104-6323, USA.

[f]Department of Materials Science and Engineering, Kwangwon National University, Samcheok 25913, South Korea.

[g]Institute of Materials Research and Engineering, A*STAR (Agency for Science, Technology, and Research), Singapore 138634, Singapore.

[h]Pohang Accelerator Laboratory, Pohang-37673, South Korea.

[i]Japan Synchrotron Radiation Research Institute (JASRI), Sayo, Hyogo 679-5198, Japan.

[j]Synchrotron X-ray Station at SPring-8, National Institute for Materials Science, 1-1-1 Koto, Sayo, Hyogo 679-5148, Japan.

[k]Laboratory for Materials and Structures, Tokyo Institute of Technology, Yokohama 226-8503, Japan.

[l]Kanagawa Institute of Industrial Science and Technology (KISTEC), Ebina 243-0435, Japan.

[m]Department of Energy and Material Science, Kyushu University, Kasuga 816-8580, Japan.

*E-mail: jyjo@gist.ac.kr

§ These authors equally contributed to this work.

Abstract

Understanding the ultra-fast dynamics of ferroelectric materials is essential for advancing the development of next-generation high speed electronic and photonic devices. In this study, we investigate the ultrafast piezoelectric response of cobalt-substituted $BiFeO_3$ ($BiFe_{1-x}Co_xO_3$) with x = 0.15, consisting of M_C and M_A type monoclinic phases. The real-time piezoelectric response in (001)-oriented $BiFe_{0.85}Co_{0.15}O_3$ (BFCO) epitaxial thin film was monitored using the time-resolved X-ray microdiffraction technique under an applied electric field with pulse widths 70 ns and 100 ns. The $BiFe_{0.85}Co_{0.15}O_3$ thin film yielded a high piezoelectric strain of approximately 0.53 % along [001] direction, with a giant c/a ratio (~ 1.26) at an electric field of 1.3 MV/cm and a pulse width of 100 ns, with a d_{33} piezoelectric coefficient of 40 pm/V. The piezoelectric response of $BiFe_{0.85}Co_{0.15}O_3$ was completely reversible on releasing the applied electric field. This finding is an important step towards the development of a high performance lead-free piezoelectric material for ultrafast operations in advanced technological applications.

Keywords: $BiFeO_3$; ultrafast piezo response; time-resolved X-ray microdiffraction

Ferroelectrics – materials which possess bi-stable polarization states depending on an applied electric field have been widely used in electronic, optical, acoustic, memory devices and neuromorphic computing applications. [1–5] In addition to their strong electromechanical coupling between polarization and strain, ultrafast operation is critical for next-generation piezoelectric/ferroelectric electronics. [3,6] The ultra-high piezoelectric response in ferroelectric materials is primarily attributed to electric field-induced polarization rotation. For instance in the classical $PbZr_{1-x}Ti_xO_3$ (PZT) at x=0.48 morphotropic phase boundary (MPB) with coexisting R and T phases, polarization rotates between $[111]_{pc}$ of R phase and $[001]_{pc}$ pseudocubic (pc) directions of T phase *via* easy paths in anisotropically flattened free energy profile [7,8]. Besides conventional Pb-based materials, highly strained $BiFeO_3$ (BFO) based compounds grown on $SrTiO_3$ and $LaAlO_3$ (LAO) substrates have been recently studied. [9–12] The undoped $BiFeO_3$ (BFO) crystallizes in the rhombohedral perovskite crystal structure (space group *R*3*c*) with the ferroelectric polarization along the $[111]_{pc}$ direction.[13,14] Moreover, the BFO thin films can also be crystallized in tetragonal (*P*4*mm* symmetry) and monoclinic (*Cc* symmetry) structures depending on the epitaxial strain.[15] A monoclinic M_C phase can be stabilized in the BFO epitaxial thin films grown on $LaAlO_3$ (LAO) substrates with a large misfit strain (~ 4.5%).[16] Furthermore, *via* chemical doping, the epitaxial films of $BiFe_{1-x}Co_xO_3$ grown on LAO can crystallize in the M_C-type monoclinic phase with a large *c/a* ratio for $0 \leq x \leq 0.1$ as well as in the M_A phase for $0.2 \leq x \leq 0.4$.[9] It is important to note that the terminology of M_A and M_C-type phases in BFCO and BFO systems are different, and are explained in the previous studies.[9]

In BFCO, at the MPB (x = 0.15), both M_C and M_A phases coexist. The polarization of the M_C phase of BFCO lies along the $[101]_{pc}$ direction while the polarization in the M_A phase is along $[111]_{pc}$ direction.[9] Both the phases on either side of the MPB are monoclinic with M_C or M_A symmetry. This M_A type monoclinic phase of BFCO is similar to the M_C type monoclinic phase

in BFO thin films but is different in the polarization orientation. The polarization in M_C type monoclinic BFO is aligned along [101] direction, while it is along [111] in M_A type monoclinic BFCO. Therefore, investigating ultrafast piezoresponse in BFCO thinfilms with MPB is crucial for understanding and optimizing their potential in high-speed switching applications. Here we report the *in situ* observation of the electric field-induced ultrafast piezoelectric response in a $BiFe_{1-x}Co_xO_3$ (BFCO) thin film with x = 0.15 using the time-resolved X-ray microdiffraction (trμXRD) technique. A maximum strain of 0.53 % was achieved at an applied electric field of 1.3 MV/cm and pulse width 100 ns.

The (001)-oriented $BiFe_{0.85}Co_{0.15}O_3$ epitaxial film with the thickness of 100 nm was grown on a (001)-oriented LAO substrate, with a $La_{0.5}Sr_{0.5}CoO_3$ layer as the bottom electrode. The epitaxial film is found to be stabilized in M_C and M_A type monoclinic phases with later as the major phase.[9] Top Pt electrodes with diameters of 100 μm were deposited on the films to analyze the thin-film capacitors. Details of the sample preparation have been discussed elsewhere.[9] The trμXRD analyses in the nanosecond timescale were carried out in a 9C beamline at the Pohang Light Source utilizing X-ray photon energy of 8 keV. A pixel array detector (PILATUS 100K) was used to record the diffracted beam. A DC electric field of up to 1.3 MV/cm was applied across the BFCO film capacitor to observe the piezoelectric strain. The unipolar electric field pulses with widths of 70 ns and 100 ns, synchronized with the clock signal of the beamline, were generated using a pulse generator (Tektronix PSPL2600C). The time-dependence of piezoelectric response was recorded using the pump-probe technique, wherein diffraction patterns were recorded while varying the delay time between the onset of the applied electric field and the recording of the diffracted X-ray pulse.

First-principles density functional theory (DFT) calculations were performed to calculate the piezoelectric coefficients d_{33} in M_A type BFO, utilising the generalized gradient

approximation-Perdew Burke Ernzerhof (GGA-PBE) functional and the projector-augmented wave method with a plane-wave basis[17,18], as implemented in the Vienna ab initio simulation package (VASP) code.[19] The PBE+U method, with an effective Hubbard interaction parameter U = 4 eV, accounted for the on-site Coulomb repulsion for Fe d electrons.[20] A 2×2×2 supercells containing 40 atoms of M_A type $BiFeO_3$ was used to accurately reproduce the G-type antiferromagnetic (AFM) order. We applied a plane-wave cutoff energy of 500 eV and the Γ-centered 4×4×4 *k*-point meshes for the Brillouin-zone integration. The calculations were fully converged in energy to 10^{-6} eV/cell and the structures are relaxed until the forces were less than 10^{-2} eV/Å.

Figure 1a shows the electric field-induced lattice expansion of BFCO along the *out-of-plane* direction, recorded by monitoring the (002) Bragg reflection of the BFCO epitaxial thin film.

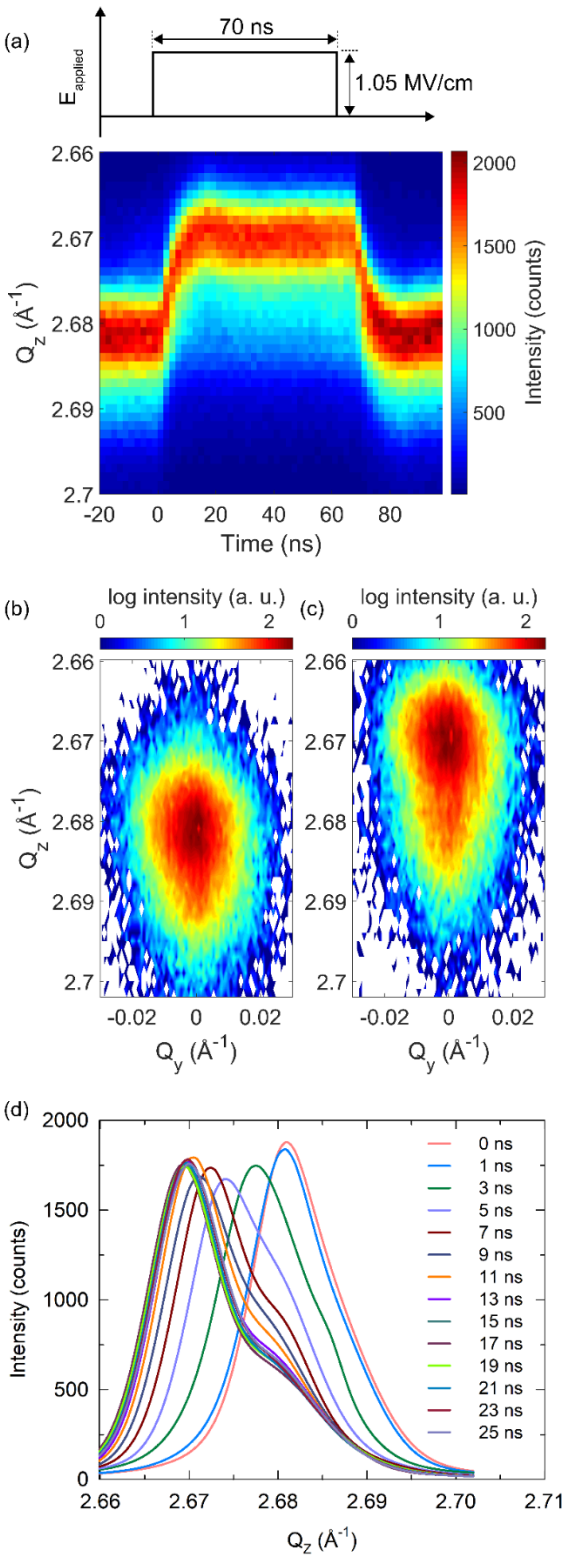


Figure 1 (a) Time-dependent diffraction pattern of BFCO observed near the (002) Bragg peak on the application of electric field (1.05 MV/cm). The panel at the top of (a) is a schematic representation of the time-dependent electric pulse applied to the sample. Reciprocal space

maps near the (002) Bragg peak at (b) E = 0 V/cm and (c) E = 1.05 MV/cm. The latter was mapped after 25 ns from the beginning of electric pulse. (d) Change of the intensity distribution around the (002) Bragg reflection with time upon the application of a 1.05 MV/cm electric field with a pulse width of 70 ns.

An electric field with a strength of 1.05 MV/cm was applied in intermittent square pulses with a width of 70 ns. The pulse shape is shown at the top panel of Figure 1a. The intensity of diffraction peaks corresponding to the M_C type monoclinic phase diminished on the application of electric field pulses, indicating a change in the phase fraction of the M_C and M_A component phases, presumably arising from the phase transition from M_C to M_A.[21] Under an electric field of 1.05 MV/cm, the *c*-axis lattice parameter was estimated to be around 4.71 Å. The time-dependent evolution of the XRD intensity distribution is shown in Figure 1d. After the electric field is turned on (E = 1.05 MV/cm), the BFCO (002) diffraction peak at Q_Z $\approx$ 2.68 Å^{-1} starts to shift and then reaches 2.67 Å^{-1} at $t \approx$ 25 ns. However, only a part of the film contributes to the shift of Bragg reflection upon the application of an ultrafast electric field pulse while the rest remained around the original position. After turning off the electric field, the (002) diffraction peaks reverted to their zero-field positions in less than 10 ns. The ultrafast piezoelectric response of BFCO epitaxial films was further investigated using time-resolved reciprocal space mapping (RSM) around the (002) Bragg reflections to analyze the lattice phases in detail. Figures 1(b-c) shows the RSMs of BFCO film at E = 0 and 1.05 MV/cm respectively, and the latter was mapped at 25 ns after the application of the electric field pulse, which further confirms that some volume fraction of the lattice expands under the application of electric field.

The change of lattice parameters was investigated in more detail by monitoring the XRD peak evolution around the {113} Bragg peaks under an applied electric field with a pulse

width of 70 ns. The time-dependent peak evolution corresponding to both the {113} reflections are shown in Figure 2a.

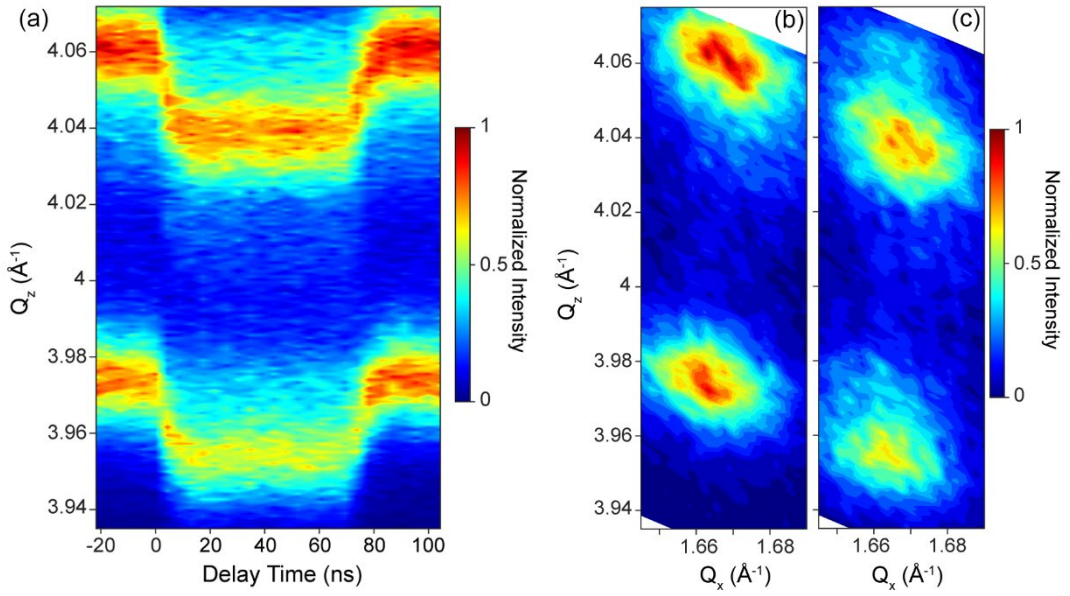


Figure 2 (a) Time-dependent diffraction patterns of BFCO near the $(\bar{1}\bar{1}3)/(\bar{1}13)$ and $(113)/(1\bar{1}3)$ Bragg peaks, on the application of a constant 1.25 MV/cm electric field for 70 ns. Reciprocal space map around the {113} reflections at (b) E = 0 MV/cm and (c) E = 1.25 MV/cm.

Under an applied electric field of 1.25 MV/cm, the peaks corresponding to both the monoclinic reflections were shifted to lower Q_z values. The RSMs corresponding to the {113} Bragg peaks were constructed before and during the applications of the nanosecond electric field pulses, as shown in Figures 2(b-c) respectively. The upper reflection corresponding to the $(\bar{1}\bar{1}3)/(\bar{1}13)$ shifted by approximately 0.4 % while the lower reflection corresponding to $(113)/(1\bar{1}3)$ shifted by approximately 0.35 %. Both {113} diffraction peaks reverted to their zero-field positions within 10 ns of the removal of applied electric field.

The experimental piezoelectric responses of BFCO thin films in the nanosecond time regime, recorded by applying 100 ns electric field pulses, are shown in Figure 3a. A maximum piezoelectric strain of 0.53 % was obtained at an applied electric field strength of 1.3 MV/cm, corresponding to the *c*/*a* ratio of 1.26. The experimental piezoelectric coefficient (d_{33}) is estimated from the linear slope of the curve, yielding a large value of 40 pm/V. The DFT calculations were performed to determine the piezoelectric response of the M_A phase to strain. The piezoelectric constant e_{33} is obtained from the strain-ΔP curve shown in Figure 3b was estimated to be in the range of 5.42 to 7.32 C/m². Using the linear relationship between the piezoelectric coefficient and the elastic constant for bulk modulus of BFO, [22,23] the piezoelectric coefficients, d_{33}, is calculated to be in the range from 39 to 53 pm/V, which is in excellent agreement with experimental value of 40 pm/V.

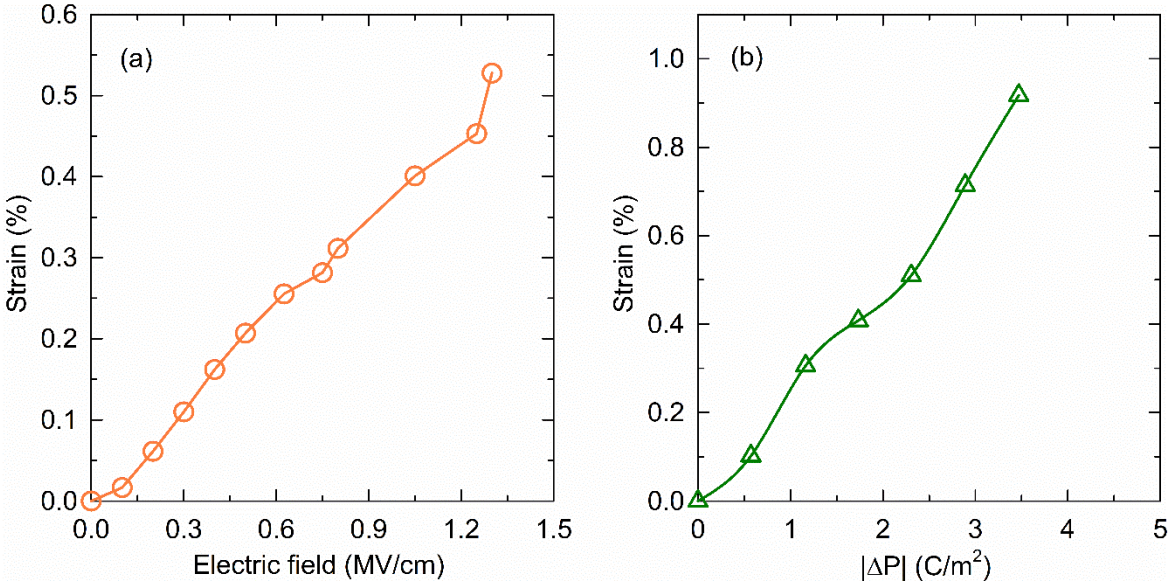


Figure 3 (a) The maximum strain as a function of applied electric field strength obtained after applying the electric field with pulse width 100 ns. (b) the strain-polarization variation curve obtained using theoretical calculations.

From an engineering perspective, the high piezoelectric response with a d_{33} value of approximately 40 pm/V and a short rise time is promising for high-speed electronics and

electromechanical actuators, since the relaxation time of piezoelectric response upon removal of the applied electric field is shorter than 10 ns for our system. Such a fast rise time, short relaxation time, and complete reversibility of ultrafast piezoelectric response enable an operation frequency as high as 4.75 MHz when using a 100 ns square pulse (period 200 ns) with a holding time of 10 ns.

In conclusion, we successfully observed the ultrafast piezoelectric response in $BiFe_{0.85}Co_{0.15}O_3$ ferroelectric epitaxial thin films under an electric field pulse with a width of 70 and 100 ns. The *c*/*a* lattice parameter ratio approached approximately 1.26 at E = 1.3 MV/cm, corresponding to the piezoelectric strain of 0.53%. This ultrafast piezoelectric response in the $BiFe_{0.85}Co_{0.15}O_3$ system will stimulate the scientific and engineering communities to further study this class of ultrafast functional materials, leading to the realization of high frequency operating electronics and actuators. Future studies can explore the ultrafast response of M_A-T MPB observed at x = 0.35–0.40 in $BiFe_{1-x}Co_xO_3$ using trμxrd. Additionally, examining the lattice dynamics and phase transition mechanisms at different time scales will provide a deeper understanding of the piezoelectric responses over the time scales ranging from nanoseconds to microseconds.

Acknowledgments

JYJ acknowledges support through grants from the National Research Foundation of Korea (NRF) funded by the Korean government (NRF- 2017M3D1A1040828, 2020R1A2C2006127, 2020K1A3A7A09080404, and 2021R1A5A1032996) and GRI (GIST Research Institute) project by GIST. SU wishes to thank the support of the Basic Science Research Program through the National Research Foundation of Korea (NRF), funded by the Ministry of Education (NRF- 2019R1I1A1A01057804) and support from Pohang Light Source. GA wishes to thank the support of the Basic Science Research Program through the National Research

Foundation of Korea (NRF), funded by the Ministry of Education (NRF-2020R1I1A1A01054253). YQ, JZ, and AMR acknowledge the support of the US Office of Naval Research, under grant N00014-20-1-2701. YQ, JZ, and AMR thank the HPCMO of the US DoD for computational support. H.J.L. acknowledges the support by 2023 Research Grant from Kangwon National University and by "Regional Innovation Strategy (RIS)" through the National Research Foundation of Korea (NRF) funded by the Ministry of Education (MOE) (2022RIS-005).

References

[1] C.T. Nelson, P. Gao, J.R. Jokisaari, C. Heikes, C. Adamo, A. Melville, S.H. Baek, C.M. Folkman, B. Winchester, Y. Gu, Y. Liu, K. Zhang, E. Wang, J. Li, L.Q. Chen, C.B. Eom, D.G. Schlom, X. Pan, Domain dynamics during ferroelectric switching, Science (1979) 334 (2011) 968–971. https://doi.org/10.1126/SCIENCE.1206980/SUPPL_FILE/NELSON.SOM.PDF.

[2] S. Li, Y. Wang, M. Yang, J. Miao, K. Lin, Q. Li, X. Chen, J. Deng, X. Xing, Ferroelectric thin films: performance modulation and application, Mater Adv 3 (2022) 5735–5752. https://doi.org/10.1039/D2MA00381C.

[3] R. Gu, V. Juvé, C. Laulhé, H. Bouyanfif, G. Vaudel, A. Poirier, B. Dkhil, P. Hollander, C. Paillard, M.C. Weber, D. Sando, S. Fusil, V. Garcia, P. Ruello, Temporal and spatial tracking of ultrafast light-induced strain and polarization modulation in a ferroelectric thin film, Sci Adv 9 (2023). https://doi.org/10.1126/SCIADV.ADI1160/SUPPL_FILE/SCIADV.ADI1160_SM.PDF.

[4] J. Li, C. Ge, J. Du, C. Wang, G. Yang, K. Jin, J. Li, C. Ge, J. Du, C. Wang, G. Yang, K. Jin, Reproducible Ultrathin Ferroelectric Domain Switching for High-Performance Neuromorphic Computing, Advanced Materials 32 (2020) 1905764. https://doi.org/10.1002/ADMA.201905764.

[5] A. Chanthbouala, V. Garcia, R.O. Cherifi, K. Bouzehouane, S. Fusil, X. Moya, S. Xavier, H. Yamada, C. Deranlot, N.D. Mathur, M. Bibes, A. Barthélémy, J. Grollier, A ferroelectric memristor, Nature Materials 2012 11:10 11 (2012) 860–864. https://doi.org/10.1038/nmat3415.

[6] M. Willatzen, Z. Lin Wang, Continuum Model for Coupled Acousto-Optical Phonons in Piezoelectric Materials, in: L.L. Bonilla, E. Kaxiras, R. Melnik (Eds.), Coupled Mathematical Models for Physical and Biological Nanoscale Systems and Their Applications, Springer International Publishing, Cham, 2018: pp. 75–93. https://link.springer.com/chapter/10.1007/978-3-319-76599-0_5.

[7] D. Damjanovic, A morphotropic phase boundary system based on polarization rotation and polarization extension, Appl Phys Lett 97 (2010) 62906. https://doi.org/10.1063/1.3479479/339464.

[8] L. Bellaiche, A. García, D. Vanderbilt, Electric-field induced polarization paths in $Pb(Zr_{1-x}Ti_3)O_3$ alloys, Phys Rev B 64 (2001) 060103. https://doi.org/10.1103/PhysRevB.64.060103.

[9] K. Shimizu, H. Hojo, Y. Ikuhara, M. Azuma, Enhanced Piezoelectric Response due to Polarization Rotation in Cobalt-Substituted $BiFeO_3$ Epitaxial Thin Films, Advanced Materials 28 (2016) 8785–8785. https://doi.org/10.1002/adma.201670277.

[10] D. Sando, B. Xu, L. Bellaiche, V. Nagarajan, A multiferroic on the brink: Uncovering the nuances of strain-induced transitions in $BiFeO_3$, Appl Phys Rev 3 (2016). https://doi.org/10.1063/1.4944558/13662291/011106_1_ACCEPTED_MANUSCRIPT.PDF.

[11] C.J. Cheng, D. Kan, V. Anbusathaiah, I. Takeuchi, V. Nagarajan, Microstructure-electromechanical property correlations in rare-earth-substituted $BiFeO_3$ epitaxial thin films at morphotropic phase boundaries, Appl Phys Lett 97 (2010). https://doi.org/10.1063/1.3520642/120529.

[12] J.Y. Lee, G. Anoop, S. Unithrattil, W.J. Seol, Y. Yeo, C.H. Yang, S.Y. Lee, J.Y. Jo, The role of intermediate S-polymorph towards high piezoelectricity in La-doped $BiFeO_3$ epitaxial thin films, Acta Mater 207 (2021) 116683. https://doi.org/10.1016/J.ACTAMAT.2021.116683.

[13] R.J. Zeches, M.D. Rossell, J.X. Zhang, A.J. Hatt, Q. He, C.H. Yang, A. Kumar, C.H. Wang, A. Melville, C. Adamo, G. Sheng, Y.H. Chu, J.F. Ihlefeld, R. Erni, C. Ederer, V. Gopalan, L.Q. Chen, D.G. Schldin, N.A. Spaldin, L.W. Martin, R. Ramesh, A strain-driven morphotropic phase boundary in $BiFeO_3$, Science (1979) 326 (2009) 977–980. https://doi.org/10.1126/science.1177046.

[14] D.G. Schlom, L.Q. Chen, C.J. Fennie, V. Gopalan, D.A. Muller, X. Pan, R. Ramesh, R. Uecker, Elastic strain engineering of ferroic oxides, MRS Bull 39 (2014) 118–130. https://doi.org/10.1557/MRS.2014.1.

[15] D. Sando, A. Barthélémy, M. Bibes, $BiFeO_3$ epitaxial thin films and devices: Past, present and future, Journal of Physics Condensed Matter 26 (2014) 473201. https://doi.org/10.1088/0953-8984/26/47/473201.

[16] H.M. Christen, J.H. Nam, H.S. Kim, A.J. Hatt, N.A. Spaldin, Stress-induced R-M A-M C-T symmetry changes in $BiFeO_3$ films, Phys Rev B 83 (2011) 144107. https://doi.org/10.1103/PhysRevB.83.144107.

[17] P.E. Blöchl, Projector augmented-wave method, Phys Rev B 50 (1994) 17953. https://doi.org/10.1103/PhysRevB.50.17953.

[18] J.P. Perdew, K. Burke, M. Ernzerhof, Generalized Gradient Approximation Made Simple, Phys Rev Lett 77 (1996) 3865. https://doi.org/10.1103/PhysRevLett.77.3865.

[19] G. Kresse, J. Furthmüller, Efficiency of ab-initio total energy calculations for metals and semiconductors using a plane-wave basis set, Comput Mater Sci 6 (1996) 15–50. https://doi.org/10.1016/0927-0256(96)00008-0.

[20] S.L. Dudarev, G.A. Botton, S.Y. Savrasov, C.J. Humphreys, A.P. Sutton, Electron-energy-loss spectra and the structural stability of nickel oxide: An LSDA+U study, Phys Rev B 57 (1998) 1505. https://doi.org/10.1103/PhysRevB.57.1505.

[21] S.J. Smith, J.M. Montgomery, Y.K. Vohra, S.G. Kim, D. Byeon, S. Singh, W. Siemons, C. Beekman, G.J. Macdougall, J.L. Zarestky, S.E. Nagler, H.M. Christen, A complete strain–temperature phase diagram for $BiFeO_3$ films on $SrTiO_3$ and $LaAlO_3$ (0 0 1) substrates, J Phys D Appl Phys 47 (2013) 034011. https://doi.org/10.1088/0022-3727/47/3/034011.

[22] S. Yasui, O. Sakata, M. Nakajima, S. Utsugi, K. Yazawa, T. Yamada, H. Funakubo, Piezoelectric properties of {100}-oriented epitaxial $BiCoO_3$-$BiFeO_3$ films measured using synchrotron X-ray diffraction, Jpn J Appl Phys 48 (2009) 09KD06. https://doi.org/10.1143/JJAP.48.09KD06/XML.

[23] Y. Nakamura, M. Kawai, M. Azuma, M. Kubota, M. Shimada, T. Aiba, Y. Shimakawa, Enhanced piezoelectric constant of (1-x)$BiFeO_3$-x$BiCoO_3$ thin films grown on $LaAlO_3$ substrate, Jpn J Appl Phys 50 (2011) 031505. https://doi.org/10.1143/JJAP.50.031505/XML.